

Effect of NiO content on the optical band gap, refractive index, and density of $\text{TeO}_2\text{-V}_2\text{O}_5\text{-NiO}$ glasses

Dariush Souri · Seyed Ali Salehizadeh

Received: 6 October 2008 / Accepted: 17 August 2009 / Published online: 26 August 2009
© Springer Science+Business Media, LLC 2009

Abstract Amorphous layers and bulk glasses of $40\text{TeO}_2\text{-(}60-x\text{)V}_2\text{O}_5\text{-}x\text{NiO}$ compositions with $0 \leq x \leq 30$ (in mol%) have been prepared using the usual blowing technique and press-melt quenching method, respectively. The optical absorption spectra of the layers have been recorded in the wavelength range 400–800 nm. The fundamental absorption edge has been identified from the optical absorption spectra. The optical band gap, width of the tail of the localized states, and refractive index have been evaluated using available theories. Results show that the values of optical band gap decrease from 2.02 to 1.64 eV as the contribution of NiO increases. The refractive index dispersion is fitted to the single oscillator model, and results show that the static refractive index increase from 1.309 to 1.673 as the NiO content increases. The glass transition temperature, density, and molar volume have been studied, indicating act of NiO as network modifier. Values of theoretical optical basicity are also reported.

Introduction

Oxide glasses containing transition metal oxides (TMOs) have been studied extensively owing to their semiconducting properties [1–7]. The structural and physical properties of the binary $\text{TeO}_2\text{-V}_2\text{O}_5$ glasses have been investigated [8–12]. There are several reports about the physical properties of ternary vanadium tellurite glassy

systems including the third component of MoO_3 [13–15], Ag_2O [16], CuO [17], Li_2O [18], BaO [19], Fe_2O_3 [20], TiO_2 [21], Bi_2O_3 [22], ZnCl_2 [23]. Tellurite glasses have interesting glass formation ability, glass structure, no hygroscopic properties, high thermal expansion coefficients, low glass transition temperature (T_g), and low melting-point [24]. Nickel oxide (NiO) is an interesting material due to its useful electronic, magnetic, and catalytic properties [25]. NiO has also become very important for it can be used as electrode material in battery systems [26]. A change in glass composition may affect the induced optical absorption due to several reasons, namely, the polarization power of network formers, modifiers, their coordination numbers, the concentration of non-bridging oxygen (oxygen ions having dangling bonds), the presence of multi-valent network forming and modifying ions [24]. Studying the optical absorption, particularly the shape and shift of the absorption edge, is a very useful technique for understanding the basic mechanism of optically-induced transitions in crystalline and non-crystalline materials, as well as providing information about the energy band structure.

Some of researchers have studied electrical conduction [27] and small polaron transport [28] in vanadium–tellurite–nickel glasses, but there is no report on their optical properties. So, we have two purposes in present work; the first is investigation of optical properties of these glasses and the second is to determine some of the structural parameters of $\text{TeO}_2\text{-V}_2\text{O}_5\text{-NiO}$ glasses such as density and optical basicity.

Experimental details

The ternary $40\text{TeO}_2\text{-(}60-x\text{)V}_2\text{O}_5\text{-}x\text{NiO}$ glasses with $0 \leq x \leq 30$ (in mol%), hereafter, termed as TVNx, were

D. Souri (✉)
Department of Physics, University of Malayer, Malayer, Iran
e-mail: d.souri@gmail.com; d.souri@malayeru.ac.ir

S. A. Salehizadeh
School of Physics, Damghan University of Basic Sciences,
Damghan, Iran

prepared by well dry mixing of 16 g batches of the high purity oxide powders V_2O_5 (MERCK, 99.99% pure), TeO_2 (BDH, 99.99% pure), and NiO (MERCK, 99.99% pure) as starting raw materials in a mortar for 15 min. Appropriate amounts of the oxide powders were weighed using a precise balance (Kern ALS 220-4, Germany) having an accuracy of 0.1 mg. Then, the mixture was pre-heated in atmospheric conditions at 400 °C for 30 min in order to dehydrate it and was melted in an alumina porcelain crucible in the temperature range 720–980 °C for 0.5 h, depending on the composition, in an electric furnace (ATBIN ALF 15) in air. The melt was mixed every 5 min to prevent the separation of the three components. The melt was poured on to a polished steel mold and immediately pressed by another polished steel block (press-melt quenching method), where the blocks were kept at room temperature. Amorphous layers of the present samples were prepared using blowing technique; in this method, the melt temperature was reduced 40 °C to increase its viscosity. A small amount of this high viscosity liquid was collected on one end of a fine borosilicate tube and was then blown into air. Thickness of produced films was in the micrometer range which is well suited for optical measurements. The thickness of glassy films was measured using a dial gauge (D.C Lutron 516). Thicknesses of the blown films were 4, 6, 18, 325, and 232 μm for TVN0, TVN5, TVN10, TVN20, and TVN30 samples, respectively. Furthermore, the films produced by blowing in to air have not any substrate, thus the optical spectra were recorded using a double-beam spectrophotometer with the air blank as reference material. The characterization of the glass systems was carried out by X-ray diffraction (XRD) studies using a Bruker diffractometer (AXS D8 Advance, CuK_α , Germany). The optical absorption spectra of the films were recorded using a GBC double beam spectrophotometer (UV/Visible 916) in the wavelength range 400–800 nm at room temperature.

The density (ρ) of each sample was calculated by the Archimedes method using para-xylene as immersion liquid [14, 29]. Also, the glass transition temperature (T_g) of these samples was obtained using differential scanning calorimetry (DSC: Pyris1, USA) which increases with increasing of NiO content and was in the range 249.3–356.3 °C. The molar volume (V_M) was calculated using the relation $V_M = M_T/\rho$, where M_T is the total molecular weight of the multicomponent system given by

$$M_T = x_{TeO_2}Z_{TeO_2} + x_{V_2O_5}Z_{V_2O_5} + x_{NiO}Z_{NiO} \quad (1)$$

where x_{TeO_2} , $x_{V_2O_5}$, and x_{NiO} are the mole fractions of the constituent oxides, and Z_{TeO_2} , $Z_{V_2O_5}$, and Z_{NiO} are the molecular weight of the different oxides.

Results and discussion

XRD characterization

As Fig. 1 shows, XRD characterization has been carried out on different samples, confirming the amorphous nature of TVN x samples; these results are in agreement with the DSC analysis which confirm the glassy nature of the present samples, i.e., see “Experimental details” section.

Optical properties

Optical gap and band tailing width

The optical absorption spectra of TVN x glass systems are shown in Fig. 2.

Figure 2 shows that the optical absorption edges are not sharp for the present glasses, which is in accord with their amorphous nature. It is also observed that the positions of

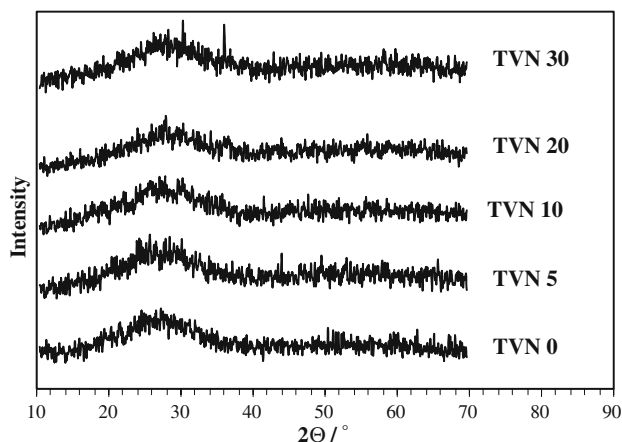


Fig. 1 XRD pattern of TVN x samples

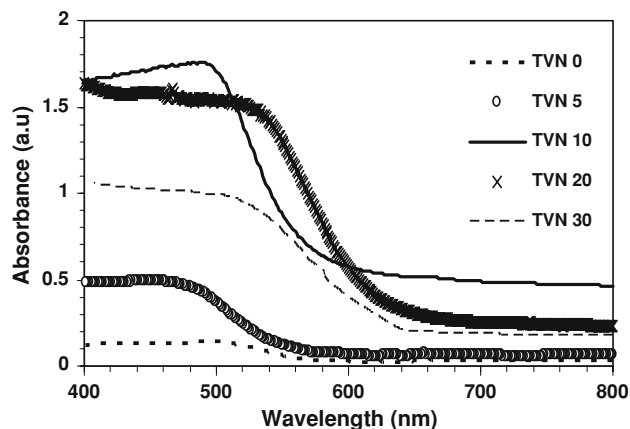


Fig. 2 Optical absorption spectra of TVN x samples

Table 1 Optical parameters of TVN_x samples

Sample	E_g (eV)	E_c (eV)	$n(0)$	ϵ_s
TVN0	2.02	0.164	1.309	1.713
TVN5	1.99	0.198	1.351	1.825
TVN10	1.83	0.284	1.487	2.211
TVN20	1.75	0.206	1.676	2.808
TVN30	1.64	0.244	–	–

the fundamental absorption edge shift toward red as the content of NiO increases (see Table 1). This shift can be due to an increase in the concentration of non-bridging oxygens (NBOs) when nickel oxide is added to TVN_x glass systems [30].

The absorption coefficient, $\alpha(\omega)$, near the edge of each spectrum has been obtained by the relation [31]:

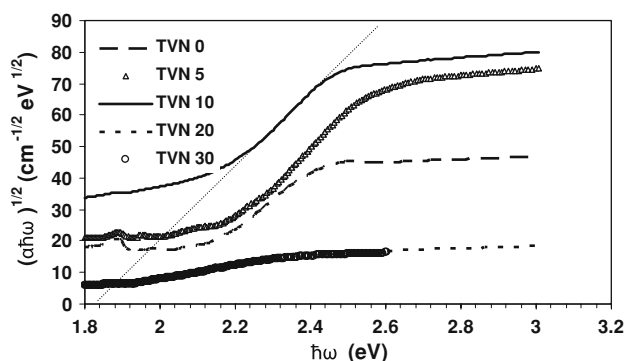
$$\alpha(\omega) = \left(\frac{1}{d}\right) \ln\left(\frac{I_0}{I_t}\right) = \frac{2.303A}{d} \quad (2)$$

where d and A are the thickness of the sample and absorbance, respectively; also I_0 and I_t are the intensities of incident and transmitted radiation, respectively. In the high absorption region, $\alpha(\omega) \geq 10^4 \text{ cm}^{-1}$, Mott and Davis proposed the following relation for amorphous materials [32]:

$$\alpha \hbar\omega = A (\hbar\omega - E_{\text{opt}})^m \quad (3)$$

where E_{opt} is the optical band gap, $\hbar\omega$ is incident photon energy, and m is the index which can have different values (1/2, 3/2, 2, and 3) corresponding to direct allowed, direct forbidden, indirect allowed, and indirect forbidden transitions, respectively. A is a constant called the band tailing parameter [29] and is related to speed of light (c), the refractive index (n), the extrapolated D.C conductivity at $T = 0 \text{ K}$ (σ_0), and the band tailing energy (E_c) [14].

The variation of $(\alpha \hbar\omega)^{1/2}$ with $\hbar\omega$ was plotted (Tauc plot) for TVN_x samples (see Fig. 3). The values of E_{opt} have been calculated by extrapolating the linear region of the curves to intercept $\hbar\omega$ at $(\alpha \hbar\omega)^{1/2} = 0$ and are presented in Table 1. By using the least squares method, it was

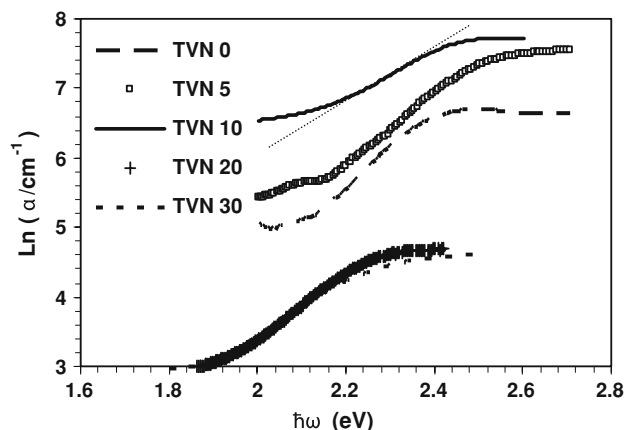
**Fig. 3** Tauc's plots for TVN_x samples

observed that the best fitting occurs for $m = 2$ (linear correlation coefficient: $R^2 = 0.9988$ – 0.9994), indicating indirect allowed transition in these glasses. In addition, as listed in Table 1, the values of E_{opt} decrease from 2.02 to 1.64 eV as the contribution of NiO increases from 0 to 30 mol% in TVN_x systems. The introduction of NiO as a network modifier brings about the formation of non-bridging oxygens simply bound by O^{2-} ions. There are more easily excited so that absorption takes place even with light of less energy, i.e., the absorption edge is shifted into the longer wavelength region (shift toward red); thus, the optical band gap values decrease with increasing in NiO content. On the other hand, NiO^{2+} ions may have the 4 and 6 coordination numbers; but formation of non-bridging oxygens can be due to the ions with coordination of 6. Therefore, increasing of NiO content causes the formation of NiO^{2+} ions with coordination of 6 and hence the formation of further NBOs.

In the low absorption region, $\alpha(\omega) < 10^4 \text{ cm}^{-1}$, the absorption coefficient follows the Urbach rule given by [14, 29]:

$$\alpha(\omega) = \alpha_0 \exp\left(\frac{\hbar\omega}{E_c}\right) \quad (4)$$

where α_0 is a constant and E_c is width of the tail of localized states (Urbach energy) corresponding to the optical transition between localized tail states in adjacent of valence band and extended state in the conduction band lying above the mobility edge. The Urbach plots (plot of $\ln \alpha$ vs. $\hbar\omega$) of the present samples are shown in Fig. 4. Therefore, using Eq. 4 and least squares method ($R^2 = 0.9987$ – 0.9993), the values of E_c , in eV, were obtained from the reciprocal of the slope of the linear region of Urbach plots; results are listed in Table 1. Upon the data of E_{opt} and E_c , the Davis–Mott model [32] of the density of states can be suggested for these glasses. The values of E_c have no certain trend. This behavior is

**Fig. 4** Urbach's plot for TVN_x samples

described by considering disorder and localized states in optical band gap of given glasses [14].

Room temperature refractive index determination

The transmittance spectra, T , of amorphous TVN x layers were measured in the wavelength range 400–800 nm. As illustrated in Fig. 5a for TVN5, the spectrum shows interference pattern with a sharp fall of transmittance at the band edge. Because of existence of this interference pattern, Swanepoel [33] represented the method based on the

approach of Manifacier [34]. In this method (single oscillator model), the refractive index $n(\lambda)$ can be calculated by creating an upper and lower envelope on the transmission spectrum beyond the absorption edge (in the region of weak absorption) as:

$$n = \sqrt{N + \sqrt{N^2 - S^2}} \tag{5}$$

where

$$N = 2S \left(\frac{T_{\max} - T_{\min}}{T_{\max} \times T_{\min}} \right) + \frac{S^2 + 1}{2} \tag{6}$$

where S is the refractive index of the substrate, T_{\min} and T_{\max} are the values of the envelope at the wavelengths in which the upper and lower envelope at the experimental transmittance spectrum are tangent, respectively [33]. The determined values of the refractive index versus wavelength plot are shown in Fig. 5b.

It is seen from the Fig. 5b that the refractive index of the TVN5 layer (and also other TVN x layers) decreases with increasing wavelength. The magnitude of the refractive index is lower than that reported for polycrystalline films and single crystals due to increasing of the lattice parameter in amorphous material [11]. The energy dependence of n of amorphous materials can be fitted to the Wemple and DiDomenico dispersion relationship (WDD model) [35] as:

$$n^2(E) - 1 = \frac{E_d E_0}{E_0^2 - E^2} \tag{7}$$

where E_0 , E_d , and E are single oscillator energy, dispersion energy (the oscillator strength which is a value of the strength of interband optical transitions) and incident photon energy ($\hbar\omega$), respectively [36]. By plotting $(n^2 - 1)^{-1}$ vs. E^2 (Fig. 5c) and fitting the data with a straight line, the slope of line and the y-axis intercept determine $-\frac{1}{E_0 E_d}$ and $\frac{E_0}{E_d}$, respectively.

The static refractive index, $n(0)$, is given by:

$$n^2(0) = 1 + \frac{E_d}{E_0}$$

The obtained values of E_0 and E_d , from Fig. 5c, for TVN5 are found to be 3.060 and 2.520 eV, respectively. The values of static dielectric constant, ϵ_s , and the values of static refractive index are listed at Table 1 indicating increase in both ϵ_s and $n(0)$ as NiO is increased.

Calculation of density and optical basicity

The values of density and molar volume have been listed in Table 2. Density of TVN x samples increases with increase in NiO content while there is a decrease in molar volume of compositions as NiO is added. As mentioned in the “Experimental details” section, T_g data increase with

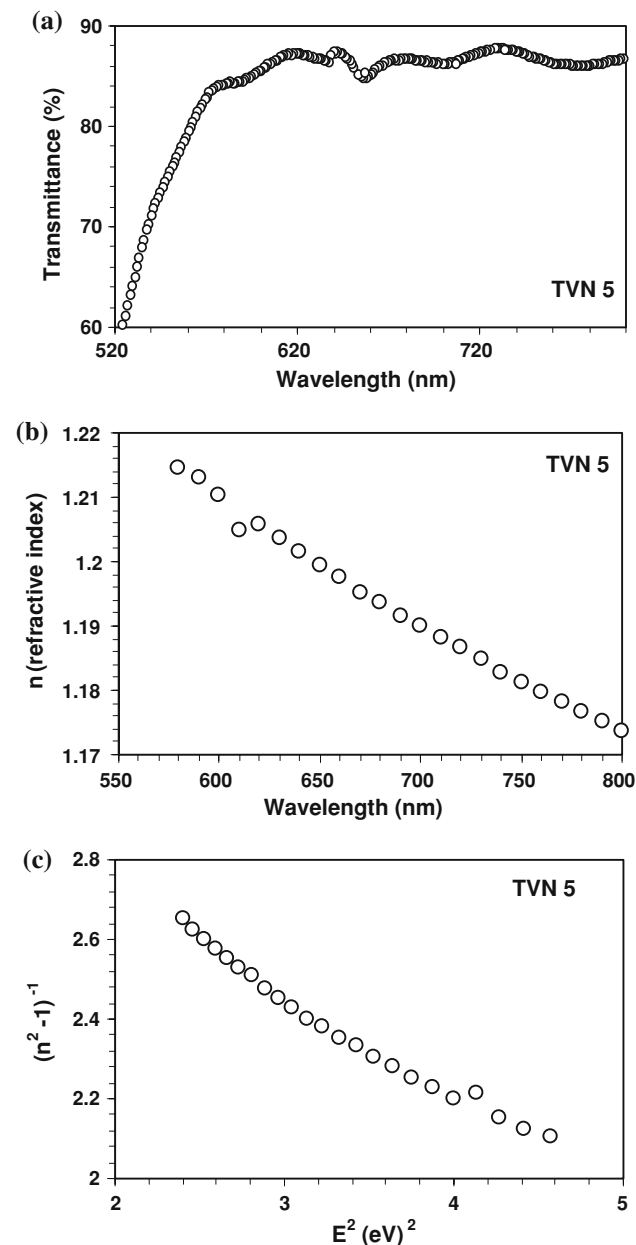


Fig. 5 a Transmission spectra for TVN5 sample. b Plot of refractive index vs. wavelength for TVN5 sample. c Plot of $(n^2 - 1)^{-1}$ vs. E^2 for TVN5 sample

Table 2 Density, optical basicity, and molar volume of TVN samples

Sample	ρ (g/cm ³)	V_m (cm ³ mol ⁻¹)	Λ_{th}
TVN0	3.856	44.858	1.014
TVN5	3.872	43.289	1.011
TVN10	3.9	41.604	1.008
TVN20	4.019	37.703	1.002
TVN30	4.243	33.189	0.994

increasing the NiO concentration, confirming the increasing of the rigidity and packing of these samples; these results confirm the increasing of the density and refractive index of the samples. The change in molar volume depends on the rates of changes of both density and molar weight. However, the rate of decrease in molar weight is greater than the rate of increase in density. The variations of density and molar volume can be explained in term of change in the structure of glasses. The same situation has been seen for other glasses [29, 37].

The theoretical optical basicity of the present glasses has been calculated for under study glasses using the relation [29, 38]:

$$\Lambda_{th} = X_{TeO_2}\Lambda_{TeO_2} + X_{V_2O_5}\Lambda_{V_2O_5} + X_{NiO}\Lambda_{NiO} \quad (8)$$

where Λ_{TeO_2} , $\Lambda_{V_2O_5}$, and Λ_{NiO} are basicities assigned to the individual oxides and X_{TeO_2} , $X_{V_2O_5}$, and X_{NiO} are the equivalent fractions based on the amount of oxygen each oxide contributes to the overall material stoichiometry [29]. Here, the values of $\Lambda_{TeO_2} = 0.915$, $\Lambda_{V_2O_5} = 1.04$, $\Lambda_{NiO} = 0.975$ have been taken from the literature [39]. As listed in Table 2, the optical basicity of TVNx compositions decreases with increase in NiO concentration.

The variation of the optical basicity with addition of NiO content can be described in terms of change in the concentration of non-bridging oxygen (NBO) and coordination number; in other word, this behavior may be explained knowing the role of NiO as a modifier and the different structural units formed in these glasses. Unfortunately, there are no reports about the structural characteristics of the present glasses; thus, for better and more detailed understanding of effect of NiO addition in TVNx glasses, it seems essential that the structural characterization to be investigated.

Conclusions

The optical absorption spectra of 40TeO₂–(60 – x)V₂O₅–xNiO glasses have been recorded in the wavelength range 400–800 nm. The fundamental absorption edge has been identified from the optical absorption spectra which shift

toward red as the content of NiO increases. Also, the optical band gap (indirect allowed transition), and width of the tail of the localized states were determined. In addition, the values of E_{opt} decrease from 2.02 to 1.64 eV as the contribution of NiO increases from 0 to 30 mol% in these glasses.

The refractive index dispersion is fitted to the single oscillator model.

The density and molar volume have been studied, indicating act of NiO as network modifier. Values of theoretical optical basicity were also reported and described in terms of change in the concentration of non-bridging oxygens (NBO) (or in better word, change in structural units formed in these proposed glasses) and role of NiO as a modifier.

References

1. Chowdari BVR, Kumari PP (1997) *J Phys Chem Solids* 58(3):515
2. Pal M, Hirota K, Tsujigami Y, Sakata H (2001) *J Phys D Appl Phys* 34:459
3. Sharma BK, Dube DC, Mansingh A (1984) *J Non Cryst Solids* 65:39
4. Murugan GS, Ohishi Y (2004) *J Non Cryst Solids* 341:86
5. Jayaseelan S, Muralidharan P, Venkateswarlu M, Satyanarayana N (2005) *Mater Sci Eng B* 118:136
6. Lin J, Huang W, Sun Z, Ray CS, Day A (2004) *J Non Cryst Solids* 336:189
7. Prasad SVGVA, Reddy MS, Veeraiha N (2006) *J Phys Chem Solids* 67:2478
8. El-Moneim AA (2002) *Mater Chem Phys* 73:318
9. Sinclair RN, Wright AC, Bachra B, Dimitriev YB, Dimitriov VV, Arnaudov MG (1998) *J Non Cryst Solids* 232–234:38
10. Chopra N, Mansingh A, Chadha GK (1990) *J Non Cryst Solids* 126:194
11. Mansingh A, Dhawan VK (1983) *J Phys C Solid State Phys* 16:1675
12. Sakida S, Hayakawa S, Yoko T (2000) *J Phys Condens Matter* 12:2579
13. Soury D (2008) *J Phys D Appl Phys* 41:105102
14. Soury D, Elahi M (2006) *Indian J Pure Appl Phys* 44:419
15. Soury D, Elahi M (2007) *Phys Scr* 75:219
16. Dimitriev Y, Ivanov Y, Dimitrov M, Lefterova ED, Angelov PV (2000) *J Mater Sci Lett* 19(17):1513
17. El-Desoky MM, Al-Assiri MS (2007) *Mater Sci Eng B* 137:237
18. Rozier P, Burian A, Cuello GJ (2005) *J Non Cryst Solids* 351:632
19. Szu S, Chang F (2005) *Solid State Ionics* 176:2695
20. El-Desoky MM (2005) *J Non Cryst Solids* 351:3139
21. El-Mallawany R, El-Khoshkhany N, Afifi H (2006) *Mater Chem Phys* 95:321
22. Rajendran V, Palanivelu N, Chaudhuri BK, Goswami K (2003) *J Non Cryst Solids* 320:195
23. Gupta S, Mansingh A (1998) *Philos Mag B* 78(3):265
24. Turkey G, Dawy M (2002) *Mater Chem Phys* 77:48
25. Wi L, Wi Y, Wei H, Shi Y, Hu C (2004) *Mater Lett* 58:2700
26. Patil PS, Kadam LD (2002) *Appl Surf Sci* 199:211
27. Sega K, Kasai H, Sakata H (1998) *Mater Chem Phys* 53:28
28. El-Desoky MM (2003) *J Mater Sci Mater Electron* 14(4):215

29. Sindu S, Sanghi S, Agarwal A, Seth VP, Kishore N (2005) *Mater Chem Phys* 90:83
30. Dayanand C, Bhikshamaiah G, Salagram M (1995) *Mater Lett* 23:309
31. Kruzeleky RV, Ukah C, Racansky D, Zukotynski S, Per JM (1990) *J Non Cryst Solids* 126:194
32. Mott NF, Davis EA (1979) *Electronic process in non-crystalline materials*. Clarendon Press, Oxford
33. Swanepoel R (1983) *J Phys E* 16:1214
34. Manificier JC, Gasiot J, Fillard JP (1976) *J Phys E* 9:1002
35. El-Kabnay N, Shaaban ER, Afify N, Abou-sehly AM (2008) *Physica B* 403:31
36. Qasrawi AF (2007) *Opt Mater* 29:1751
37. Sindu S, Sanghi S, Agarwal A, Sonam K, Seth VP, Kishore N (2005) *Physica B* 365:65
38. Dimitrov V, Komatsu T (2005) *J Solid State Chem* 178:831
39. Dimitrov V, Komatsu T (2002) *J Solid State Chem* 163:100